

Design, Synthesis, Biological Evaluation, and Docking Study of Novel 4-Anilinoquinazolines Derivatives as Anticancer Agents

Azmian Moghadam, Fatemeh; Kefayati, Hassan

Department of Chemistry, Faculty of Science, Rasht Branch, Islamic Azad University, Rasht, I.R. I.R. IRAN

Evazalipour, Mehdi

Department of Pharmaceutical Biotechnology, School of Pharmacy, Guilan University of Medical Sciences, Rasht, I.R. IRAN

Ghasemi, Saeed*⁺

Department of Medicinal Chemistry, School of Pharmacy, Guilan University of Medical Sciences, Rasht, I.R. IRAN

ABSTRACT: Epidermal Growth Factor Receptor (EGFR) and Vascular Endothelial Growth Factor Receptor (VEGFR) as appropriate targets for cancer therapy have recently made a noteworthy field since the introduction of vandetanib as a dual inhibitor of VEGFR and EGFR tyrosine kinases (TKIs). In this study, twelve quinazoline derivatives were designed, synthesized, and evaluated for their cytotoxicity on A431 (human carcinoma cell) as well as HU02 (Foreskin fibroblast) cell lines by MTT assay. The binding mode of the most potent compound (**8a**) with EGFR and VEGFR2 was studied using molecular docking. Most of the compounds showed significant inhibition of the growth of A431 cells at a concentration lower than 100 μM . The compound **8a** bearing diethylamine along with 4-bromo-2-fluoroaniline exhibited the best cytotoxic activity ($\text{IC}_{50}=2.62 \mu\text{M}$) compared to erlotinib and vandetanib as positive controls. Synthesized compounds did not indicate significant cytotoxicity against HU02 cell line. The compound **8a** indicated binding energies of -6.39 and -8.24 kcal/mol as well as inhibition constants of 20.67 μM and 0.9 μM with EGFR and VEGFR-2, respectively, which showed the effective binding with VEGFR-2. The higher potency of **8a** may be put down to the flexibility of diethylamine and its higher lipophilicity as well as lower steric hindrance of this substituent.

KEYWORDS: Synthesis; Cytotoxicity; 4-anilinoquinazoline; Docking.

INTRODUCTION

Cancer is one of the most frequent causes of death all over the world. New anticancer drugs are always needed because of issues with existing compounds such as toxicity, drug resistance, and lack of appropriate potency [1-7]. The epidermal growth factor receptor (EGFR; ErbB-1; HER1 in humans), ErbB2 (HER-2/neu), ErbB3 (HER3),

and ErbB4 (HER4) are members of the ErbB receptor family. EGFR is a Receptor Tyrosine Kinase (RTK) which plays a critical role in cell-related processes such as cell survival, proliferation, migration, adhesion, and differentiation [8,9]. It is overexpressed in different solid tumors. So, it can be considered a key target for cancer

* To whom correspondence should be addressed.

+ E-mail: ghasemi_saeed@yahoo.com & ghasemi_s@gums.ac.ir
1021-9986/2022/2/353-367 15/\$/6.05

treatment. Lapatinib (TykerbTM), gefitinib (IressaTM), and erlotinib (TarcevaTM) were EGFR tyrosine kinase inhibitors (TKIs), which can lead to a dramatic decrease in the volume of the tumor. Lapatinib is a potent dual inhibitor of ErbB-1 and ErbB-2 and was approved by the United States Food and Drug Administration (FDA) for the treatment of breast cancer in 2007. In addition, Gefitinib and erlotinib received FDA approval for the treatment of non-small-cell lung cancer (NSCLC) in 2005. Various 4-anilinoquinazoline derivatives are still under investigation in clinical trials for treating cancer [10-12]. Besides, the tumor requires angiogenesis to continue its growth and invasion. The signal transmission for angiogenesis is done using the Vascular Endothelial Growth Factor Receptor (VEGFR) as a receptor tyrosine kinase. Inhibition of VEGFR stops angiogenesis of the tumor which can be an additional mechanism for cancer treatment with beneficial therapeutic effects. Vandetanib (ZD6474), an anticancer drug that is in phase III clinical trial, was introduced to inhibit both EGFR and VEGFR [13,14]. So far, various molecular scaffolds with EGFR and VEGFR inhibitory activities have been synthesized, and among them, quinazoline derivatives have drawn a lot of interest due to their different biological effects, especially as potent kinase inhibitors. Among all FDA-approved EGFR TKIs or ones under clinical trials, the 4-anilinoquinazoline-based derivatives have attracted the attention of scientists because of their potent inhibitory effect, and most of them were approved for the treatment of various kinds of malignancies [13,15]. As is presented in Figure 1, competitive inhibitors of EGFR and VEGFR-2 with 4-anilinoquinazoline scaffold can inhibit the tyrosine kinase activity of these receptors via interaction with the adenosine triphosphate (ATP) binding site of the tyrosine kinase domains [16-18]. Structure-Activity Relationship (SAR) investigation of 4-anilinoquinazoline showed that substitution of the aniline ring using large lipophilic and electron-withdrawing groups such as chlorine or bromine were preferred at the C-3' and C-4' positions while at the ortho position, small substituents such as fluorine and hydrogen are more preferable. Investigation of the quinazoline C-6 and C-7 positions showed that a wide range of substituents such as neutral, basic, and heteroaromatic side chains at C-7 position resulted in potent compounds, whereas any changes at the C-6 is more restricted and methoxy at this position is preferred [19,20]. 4-anilinoquinazoline

scaffolds with the basic side chains at C-7 position show high inhibitory activity on both EGFR and VEGFR tyrosine kinases in both in vitro and in vivo studies which may inhibit the process of angiogenesis [18,21].

Since the development of a new pharmaceutical is very costly and time-consuming, Computer-Aided Drug Discovery (CADD) methods such as Quantitative Structure-Activity Relationship (QSAR) and molecular docking have been extensively used in drug development for the prediction of potential molecular targets, which may reduce this process significantly. Among different molecular modeling methods, docking can predict the binding orientation of drug candidates to various macromolecules for the formation of a stable complex. Understanding of this orientation may be employed for the prediction of the strength of target-ligand interaction by scoring functions in order to synthesize more potent compounds [22,23].

In this study, some novel and previously synthesized 4-anilinoquinazoline compounds were designed and synthesized, with various substituted aniline rings and basic side chains at C-4 and C-7 positions of the quinazoline core, respectively, on the basis of the structures of erlotinib and vandetanib as lead compounds (Fig. 2). The synthesized compounds were evaluated for their cytotoxicity against A431 human skin cancer (Epidermoid carcinoma) cell line as an EGFR overexpressed cancer cell line and HU02 (human foreskin fibroblast) as a healthy cell line by MTT assay. Moreover, in this work, docking studies were done by AutoDock software on the crystal structure of EGFR and VEGFR tyrosine kinase domains to investigate the binding mode of compounds and design more efficient anticancer agents.

EXPERIMENTAL SECTION

Chemistry

All reagents and solvents were purchased from Merck and Sigma Aldrich. An Electrothermal-9100 melting point apparatus was used for the measurement of the melting point and are uncorrected. The InfraRed (IR) spectra were recorded on FT-IR Perkin-Elmer Spectrum Two spectrophotometer which is equipped with the Universal Attenuated Total Reflectance (UATR) with a ZnSe-Diamond composite crystal. ¹HNMR and ¹³CNMR spectra were recorded on Bruker unity 500 and 400 MHz spectrometers and chemical shifts (δ) are reported in parts per million (ppm) using tetramethylsilane (TMS)

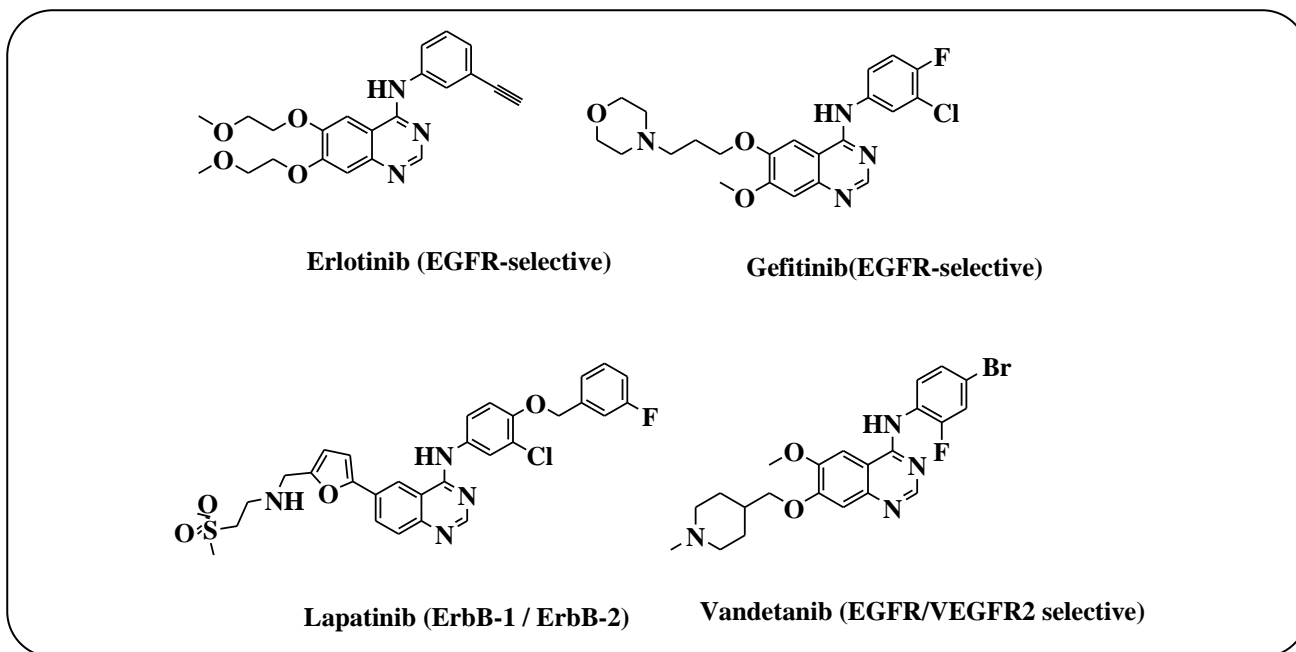


Fig. 1: Structures of EGFR tyrosine kinase inhibitors.

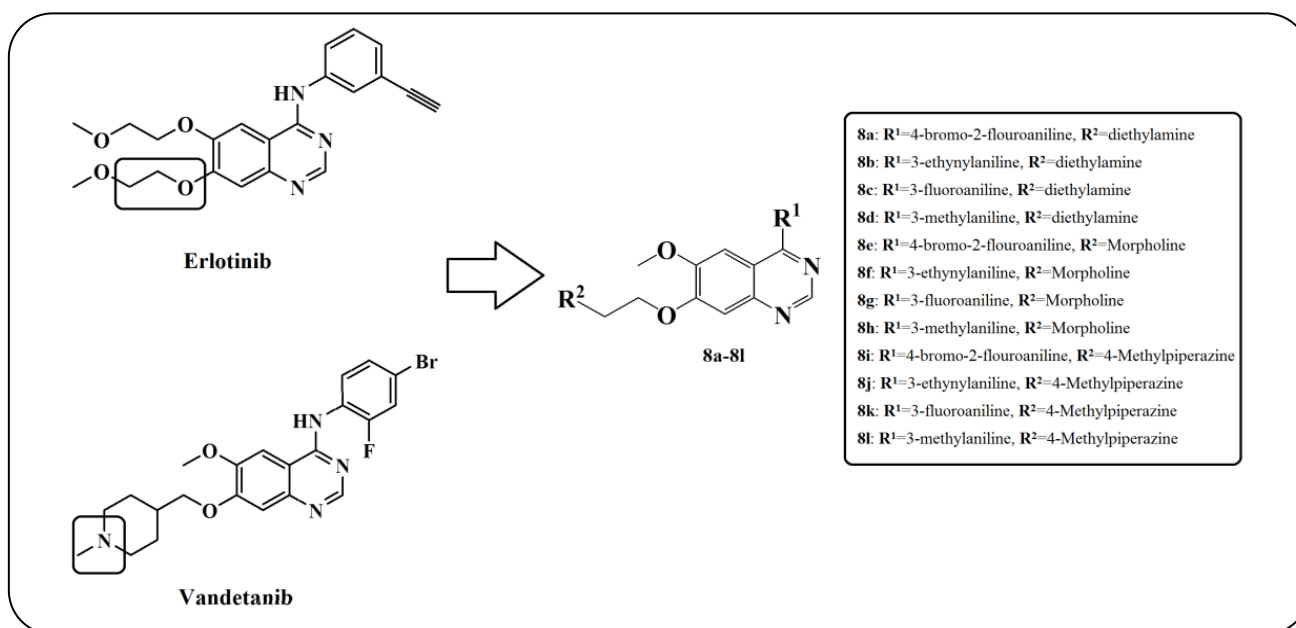


Fig. 2: The design strategy of novel compounds.

as an internal standard. Perkin Elmer 2400 with an automatic elemental analyzer was used for elemental analysis and the results were within ± 0.5 of the calculated values. The mass spectra were run on an Agilent 5973 mass spectrometer at 70 eV. Analytical TLC has performed on Merck silica gel 60 F254 plates. Silica gel 60 (Merck, particle size 0.06–0.20 mm) was used for column chromatography.

Methyl 4-hydroxy-3-methoxybenzoate (1)

Thionyl chloride (1.09 mL, 15 mmol) was added to a solution of vanillic acid (1.68 g, 10 mmol) in dry methanol (15 mL) dropwise at 0°C over 10 minutes. The mixture was stirred at room temperature overnight. The MeOH was evaporated under reduced pressure. H₂O (10 mL) was added to the residual, and the mixture was extracted by EtOAc (3×10 mL). The EtOAc layer

was dried over Na₂SO₄ and concentrated to give a white precipitate [10,24].

Yield: 69%; mp=125-127°C; IR (KBr, cm⁻¹) v_{max}: 3537(OH), 1698(C=O), 3025(C-H benzene). ¹HNMR (DMSO-*d*₆, 500 MHz): δppm 7.45 (d, J=8.5 Hz, 1H, H-C₆ phenyl), 7.42(d, J=2 Hz, 1H, H-C₂ phenyl), 6.8 (d, J=8 Hz, 1H, H-C₅ phenyl), 3.80(s, 3H, OCH₃), 3.78 (s, 3H, COOCH₃). ¹³CNMR (DMSO-*d*₆, 125 MHz) δppm 166.5, 152.1, 147.8, 123.8, 120.7, 115.6, 112.8, 56.0, 52.13. MS (ESI): m/z 182.2 [M+H]⁺.

Methyl 4-(2-chloroethoxy)-3-methoxybenzoate (2)

The mixture of **1** (1.52 g, 10 mmol), potassium carbonate (2.76 g, 20 mmol), and a catalytic amount of tetrabutylammonium bromide (TBAB) was refluxed in 20 ml of methanol for 20 min. Then, 1-bromo-2-chloroethane (2.86 g, 20 mmol) was added to the mixture. The mixture was refluxed for 4 hours. It was cooled at room temperature and the precipitate was filtered and washed with acetonitrile (2×5 mL). The filtered solution was evaporated under reduced pressure and dried to give the expected product [10,24-27].

Yield: 82%; mp=115-117.3°C; IR (KBr, cm⁻¹) v_{max}: 1705(C=O), 1512(CH₃O). ¹HNMR (DMSO-*d*₆, 500 MHz): δppm 7.56 (d, J=8.5 Hz, 1H, H-C₆ phenyl), 7.46 (s, 1H, H-C₂ phenyl), 7.09 (d, J=8.5, 1H, H-C₅ phenyl), 4.38 (t, J=5.5 Hz, 2H, ClCH₂), 4.31 (t, J=5 Hz, 2H, OCH₂), 3.97 (t, J=5 Hz, 2H, ClCH₂), 3.82(s, 3H, OCH₃), 3.81 (s, 3H, COOCH₃). ¹³CNMR (DMSO-*d*₆, 125 MHz) δppm 166.3, 152.0, 148.9, 123.4, 122.8, 112.9, 112.5, 69.1, 56.0, 52.3, 43.2. MS (ESI): m/z 244.2 [M+H]⁺.

Methyl 4-(2-chloroethoxy)-5-methoxy-2-nitrobenzoate (3)

To a solution of **2** (0.61 g, 2.5 mmol) in dry acetonitrile (5 mL) was added a mixture of HNO₃ (5 mL, 65%) and H₂SO₄ (5 mL, 98%) dropwise at 0-5 °C. This mixture was stirred below 10 °C for about 6 h, and then slowly poured into ice water (5 mL). The acetonitrile layer was washed with saturated sodium bicarbonate (2 × 5 mL) and brine (2 × 5 mL) and dried over Na₂SO₄. The solvent was concentrated under reduced pressure and the residue was dried to give a yellow solid [10,24,26,28].

Yield: 86%; mp=119-120°C; IR (KBr, cm⁻¹) v_{max}: 1715 (C=O), 1520(NO₂). ¹H NMR (DMSO-*d*₆, 500 MHz): δppm 7.67 (s, 1H, H-C₃ phenyl), 7.34 (s, 1H, H-C₆ phenyl), 4.42 (t, J=5 Hz, 2H, OCH₂), 3.98 (t, J=5 Hz, 2H,

ClCH₂), 3.93 (s, 3H, OCH₃), 3.82(s, 3H, COOCH₃). ¹³CNMR (DMSO-*d*₆, 125 MHz) δppm 165.8, 152.8, 149.2, 141.0, 121.4, 111.9, 109.2, 69.8, 57.0, 53.5, 43. MS (ESI): m/z 289.1 [M+H]⁺.

Methyl 4-(2-chloroethoxy)-2-amino-5-methoxybenzoate (4)

A mixture of **3** (0.19 g, 0.667 mmol), powdered iron (0.13 g, 2.33 mmol), and NH₄Cl (0.177 g, 3.34 mmol) in MeOH/H₂O (5 mL/2.5 mL) was refluxed for 4.5 h. The reaction mixture was cooled to room temperature and the precipitate was filtered. The filter cake was washed with chloroform. The filtrate was extracted with chloroform (3 × 15 mL) and dried over Na₂SO₄. The solvent was evaporated and the residue was purified by column chromatography with ethyl acetate/hexanes as eluent (30:70, v:v) to give the yellowish-brown product [10,24,26,28].

Yield: 68%; mp=108-107°C; IR (KBr, cm⁻¹) v_{max}: 3473, 3360 (NH₂), 1514(CH₂O), 1203 (CH₃O). ¹HNMR (DMSO-*d*₆, 500 MHz): δppm 7.15(s, 1H, H-C₆ phenyl), 6.37 (s, 1H, H-C₃ phenyl), 4.19 (t, J=5 Hz, 2H, OCH₂), 3.96 (t, J=5 Hz, 2H, ClCH₂), 3.74 (s, 3H, OCH₃), 3.66 (s, 3H, COOCH₃). ¹³CNMR (DMSO-*d*₆, 125 MHz) δppm 165.8, 152.8, 149.0, 121.4, 111.9, 109.1, 69.8, 57.0, 53.5, 43.0. MS (ESI): m/z 259.1 [M+H]⁺.

7-(2-chloroethoxy)-6-methoxyquinazolin-4(3H)-one (5)

A solution of **4** (0.1 g, 0.33 mmol) and formamidine acetate (57 mg, 0.55 mmol) in 10 mL absolute ethanol was refluxed for 6 h. The mixture was cooled to 0°C and the precipitate was filtered, washed with cold ethanol, and dried to give the white product [10,24,26].

Yield: 81%; mp=252-254°C; IR (KBr, cm⁻¹) v_{max}: 1675 (C=O), 1491(CH₂O), 1262 (CH₃O). ¹HNMR (DMSO-*d*₆, 400 MHz): δppm 8.00 (s, 1H, H-C₂ Quinazoline), 7.48 (s, 1H, H-C₈ Quinazoline), 7.17 (s, 1H, H-C₅ Quinazoline), 4.48 (t, J=5.2 Hz, 2H, ClCH₂), 4.42 (t, J=4.8 Hz, 2H, OCH₂), 4.02 (t, J=4.8 Hz, 2H, ClCH₂), 3.90 (s, 3H, OCH₃). ¹³CNMR (DMSO-*d*₆, 100 MHz) δppm 160.5, 153.5, 148.9, 145.1, 144.4, 116.4, 109.5, 105.7, 69.3, 56.2 43.2. MS (ESI): m/z 254.1 [M+H]⁺.

7-(2-chloroethoxy)-4-chloro-6-methoxyquinazoline (6)

Oxalyl chloride (0.33g, 2.63 mmol) and a catalytic amount of dimethylformamide (DMF) were added dropwise

to a solution of **5** (0.136 g, 0.527 mmol) in dichloromethane (2 mL) and stirred at room temperature for 2 days. Chloroform (10 mL) was added to the reaction mixture and neutralized with saturated sodium bicarbonate. The organic phase was separated and dried over Na₂SO₄. The solvent was evaporated to give product **6** as a yellow solid [26,29].

Yield: 88%; mp=142-144°C; IR (KBr, cm⁻¹) v_{max}: 1675 (C=O), 1491(CH₂O), 1262 (CH₃O). ¹HNMR (DMSO-*d*₆, 400 MHz): δppm 8.88 (s, 1H, H-C₂ Quinazoline), 7.48 (s, 1H, H-C₈ Quinazoline) 7.38 (s, 1H, H-C₅ Quinazoline), 4.54(t, J=4.8 Hz, 2H, OCH₂), 4.08 (t, J=4.8 Hz, 2H, ClCH₂), 4.02 (s, 3H, OCH₃). ¹³CNMR (DMSO-*d*₆, 100 MHz) δppm 158.4, 155.7, 152.6, 151.6, 148.8, 119.2, 108.2, 102.9, 69.8, 56.6, 43.0. MS (ESI): 273 [M+H]⁺.

General procedure for the synthesis of 7a-7d

A solution of **6** (0.1 g, 0.36 mmol) and proper aniline (0.73 mmol) including 4-bromo-2-fluoroaniline, 3-ethynylaniline, 3-fluoroaniline, and 3-methylaniline in isopropanol (5 mL) was refluxed for 3 h. The reaction mixture was cooled to 0°C and the precipitate was filtered, washed with cold isopropanol (5 mL), and dried to obtain **7a-7d** products [10,30]:

7-(2-chloroethoxy) -N- (4-bromo-2-fluorophenyl) -6-methoxyquinazolin-4-amine (7a)

Yield: 92%; mp=242.1-244.3°C; IR (KBr, cm⁻¹) v_{max}: 3267 (NH-aniline), 1498(CH₂O), 1228(CH₃O), 778(C-Cl). ¹HNMR (DMSO-*d*₆, 500 MHz): δppm 12.00 (s, 1H, H-N aniline), 8.84 (s, 1H, H-C₂ quinazoline), 8.51 (s, 1H, H-C₅ quinazoline), 7.78 (d, J= 8 Hz, 1H, H-C₈ quinazoline), 7.75 (s, 1H, H-C₃ aniline), 7.56(s, 1H, H-C₅ aniline), 7.48 (s, 1H, H-C₆ aniline), 4.50 (brs, 2H, OCH₂), 4.11(brs, 2H, ClCH₂), 4.05(s, 3H, OCH₃). ¹³CNMR (DMSO-*d*₆, 125 MHz) δppm 159.4, 158.5, 156.0, 155.6, 150.7, 149.2, 135.8, 130.4, 128.4, 124.5, 120.7, 107.7, 105.0, 100.9, 69.9, 57.6, 42.8. MS (ESI): m/z 427 [M+H]⁺.

7-(2-chloroethoxy) -N- (3-ethynylphenyl) -6-methoxyquinazolin-4-amine (7b)

Yield: 93%; mp=250-252°C; IR (KBr, cm⁻¹) v_{max}: 3364 (NH-anilin), 1425 (CH₂O), 1228 (CH₃O), 1157 (C-C), 775 (C-Cl). ¹HNMR (DMSO-*d*₆, 400 MHz): δppm 11.34 (s, 1H, H-N aniline), 9.04(s, 1H, H-C₂

quinazoline), 8.43 (s, 1H, H-C₅quinazoline), 8.07 (s, 1H, H-C₂ aniline), 7.97 (d, J=10 Hz, 1H, H-C₆ aniline), 7.71(t, J=7.5Hz, 1H, H-C₅ aniline), 7.60(d, J=7.5 Hz, 1H, H-C₄ aniline), 7.52 (s, 1H, H-C₈ quinazoline), 4.68 (s, 2H, OCH₂), 4.48 (s, 1H, CH ethynyl), 4.28 (s, 2H, ClCH₂), 4.23 (s, 3H, OCH₃). ¹³CNMR (DMSO-*d*₆, 100 MHz) δppm 158.2, 155.2, 153.4, 149.6, 142.7, 132.1, 128.4, 127.6, 125.8, 122.9, 111.0, 109.4, 98.9, 94.9, 88.8, 69.9, 57.4, 47.8, 42.6. MS (ESI): 353.1 [M+H]⁺.

7-(2-chloroethoxy)-N-(3-fluorophenyl)-6-methoxyquinazolin-4-amine (7c)

Yield: 94%; mp=253.6-255.3°C; IR (KBr, cm⁻¹) v_{max}: 3219 (NH-anilin), 1447 (CH₂O), 1275 (CH₃O), 755 (C-Cl). ¹HNMR (DMSO-*d*₆, 400 MHz): δppm 11.78 (s, 1H, H-N aniline), 8.89 (s, 1H, H-C₂ quinazoline), 8.53 (s, 1H, H-C₅ quinazoline), 7.79 (d, J=13.5 Hz, 1H, H-C₆ aniline), 7.67 (d, J=10 Hz, 1H, H-C₂ aniline), 7.52 (dd, J=10 Hz, 1H, H-C₅ aniline), 7.43 (s, 1H, H-C₈ quinazoline), 7.16 (t, J=9 Hz, 1H, H-C₄ aniline), 4.47 (brs, 2H, OCH₂), 4.09 (t, J=5 Hz, 2H, ClCH₂), 4.06 (s, 3H, OCH₃). ¹³CNMR (DMSO-*d*₆, 100 MHz) δppm 161.0, 158.6, 155.4, 150.6, 149.2, 139.1, 135.9, 130.7, 121.0, 113.3, 112.1, 108.2, 105.0, 101.1, 69.86, 57.7, 42.8. MS (ESI): 346.1 [M+H]⁺.

7-(2-chloroethoxy) -6- methoxy -N- m-tolylquinazolin -4-amine (7d)

Yield: 92%; mp=250-252°C; IR (KBr, cm⁻¹) v_{max}: 3219(NH-aniline), 1443 (CH₂O), 1249 (CH₃O), 773 (C-Cl). ¹HNMR (DMSO-*d*₆, 400 MHz): δppm 11.38 (s, 1H, H-N aniline), 8.93 (s, 1H, H-C₂ quinazoline), 8.41 (s, 1H, H-C₅quinazoline), 7.60 (s, 1H , H-C₈ quinazoline), 7.61(s, 1H, H-C₆ aniline), 7.50 (s, 1H, H-C₅ aniline), 7.48 (s, 1H, H-C₂ aniline), 7.26 (s, 1H, H-C₄ aniline), 4.60 (brs, 2H, OCH₂), 4.21 (s, 2H, ClCH₂), 4.15 (s, 3H, OCH₃), 2.49 (s, 3H, CH₃ aniline). ¹³CNMR (DMSO-*d*₆, 100 MHz) δppm 155.4, 153.4, 149.6, 142.7, 138.7, 137.4, 135.5, 129.2, 127.6, 125.8, 122.5, 111.5, 108.3, 104.8, 69.9, 57.5, 43.7, 21.6. MS (ESI): 343 [M+H]⁺.

General procedure for the synthesis of 8a-8l

A mixture of **7** (0.26 mmol), potassium iodide (10 mg), DMF (1 mL), and a secondary amine (Diethylamine, morpholine, and N-methylpiperazine) was refluxed for 2 h. The reaction mixture was cooled to room

temperature and crushed ice were added to the mixture. Then the mixture was extracted by chloroform (3×5), washed with saturated sodium bicarbonate and brine, and dried over Na₂SO₄. The organic layer was evaporated under reduced pressure. The final products were purified using silica gel column chromatography (elution with ethyl acetate/hexanes (4 : 6; v : v)) [24,31-33].

7-(2-(diethylamino)ethoxy)-N-(4-bromo-2-fluorophenyl)-6-methoxyquinazolin-4-amine (8a)

Yield: 36%; mp=230-231°C; IR (KBr, cm⁻¹) v_{max}: 3413 (NH aniline), 1501 (CH₂O), 1300 (CH₃O). ¹HNMR (DMSO-*d*₆, 500 MHz): δppm 9.65 (s, 1H, H-N aniline), 8.34 (s, 1H, H-C₂ quinazoline), 7.82 (s, 1H, H-C₅ quinazoline), 7.65 (d, J=9 Hz, 1H, H-C₃ aniline), 7.52 (brs, 1H, H-C₈ quinazoline), 7.46(d, J=7.5 Hz, 1H, H-C₅ aniline), 7.20 (d, J=9.5 Hz, 1H, H-C₆ aniline), 4.18 (brs, 2H, OCH₂), 3.93 (s, 3H, OCH₃), 2.86 (brs, 2H, NCH₂), 2.59 (d, J=6.5 Hz, 4H, H-CH₂ diethylamine), 2.17 (s, 3H, CH₃ aniline), 1.00 (t, J=7 Hz, 6H, CH₃ diethylamine). ¹³CNMR (DMSO-*d*₆, 125 MHz) δppm 156.8, 155.6, 153.6, 152.8, 149.0, 146.9, 129.4, 127.4, 127.42, 119.3, 119.1, 107.68, 107.64, 102.12, 102.1, 102.0, 67.28, 56.1, 50.9, 47.0, 11.86. MS (ESI): m/z 462 [M+H]⁺. Anal. Calcd for C₂₁H₂₄BrFN₄O₂: C, 54.44; H, 5.22; N, 12.09. Found: C, 54.66; H, 5.23; N, 12.03.

7-(2-(diethylamino)ethoxy)-N-(3-ethynylphenyl)-6-methoxyquinazolin-4-amine (8b)

Yield: 35%; mp=224-226°C; IR (KBr, cm⁻¹) v_{max}: 3480(NH aniline), 1450 (CH₂O), 1284 (CH₃O), 2150 (ethynyl). ¹HNMR (DMSO-*d*₆, 500 MHz): δppm 9.51 (s, 1H, H-N aniline), 8.49 (s, 1H, H-C₂ quinazoline), 8.24 (s, 1H, H-C₅ quinazoline), 7.99 (s, 1H, H-C₂ aniline), 7.90 (d, J=9.5 Hz, 1H, H-C₆ aniline), 7.83(t, J=7 Hz, 1H, H-C₅ aniline), 7.41(t, J=8 Hz, 1H, H-C₄ aniline), 7.21 (s, 1H, H-C₈ quinazoline), 4.18 (brs, 2H, OCH₂), 3.96 (s, 3H, OCH₃), 2.86 (brs, 2H, NCH₂), 2.58 (d, J=6.5 Hz, 4H, CH₂ diethylamine), 2.35 (s, 1H, CH ethynyl), 0.99 (t, J=6 Hz, 6H, CH₃ diethylamine). ¹³CNMR (DMSO-*d*₆, 125 MHz) δppm 158.7, 156.1, 149.9, 145.9, 140.9, 134.5, 132.3, 129.7, 122.2, 113.9, 108.3, 96.4, 88.4, 80.9, 67.0, 62.4, 53.4, 48.1, 10.8. MS (ESI): m/z 390.4 [M+H]⁺. Anal. Calcd for C₂₃H₂₆N₄O₂: C, 70.75; H, 6.71; N, 14.35. Found: C, 70.43; H, 6.73; N, 14.39.

7-(2-(diethylamino)ethoxy)-N-(3-fluorophenyl)-6-methoxyquinazolin-4-amine (8c)

Yield: 32%; mp=219-220°C; IR (KBr, cm⁻¹) v_{max}: 3493 (NH aniline), 1497 (CH₂O), 1210 (CH₃O). ¹HNMR (DMSO-*d*₆, 500 MHz): δppm 9.56 (s, 1H, H-N aniline), 8.52 (s, 1H, H-C₂ quinazoline), 8.15 (s, 1H, H-C₅ quinazoline), 7.89 (d, J=13 Hz, 1H, H-C₆ aniline), 7.86 (s, 1H, H-C₂ aniline), 7.62(d, J=5.5 Hz, 1H, H-C₅ aniline), 7.42 (d, J=7.5 Hz, 1H, H-C₄ aniline), 7.23 (s, 1H, H-C₈ quinazoline), 4.24 (brs, 2H, OCH₂), 3.97 (s, 3H, OCH₃), 2.97 (brs, 2H, NCH₂), 2.68 (d, J=7 Hz, 4H, CH₂ diethylamine), 1.02 (d, J=6.5 Hz, 6H, CH₃ diethylamine). ¹³CNMR (DMSO-*d*₆, 125 MHz) δppm 156.6, 153.2, 149.9, 147.7, 136.8, 130.9, 130.4, 120.1, 118.0, 110.1, 109.2, 109.0, 108.6, 102.7, 67.4, 57.0, 51.4, 47.7, 12.0. MS (ESI): m/z 384.4 [M+H]⁺. Anal. Calcd for C₂₁H₂₅FN₄O₂: C, 65.61; H, 6.55; N, 14.57. Found: C, 65.80; H, 6.56; N, 14.52.

7-(2-(diethylamino)ethoxy)-6-methoxy-N-m-tolylquinazolin-4-amine (8d)

Yield: 34%; mp=222-223.9 °C; IR (KBr, cm⁻¹) v_{max}: 3278 (NH aniline), 1417 (CH₂O), 1305 (CH₃O). ¹HNMR (DMSO-*d*₆, 500 MHz): δppm 9.46 (s, 1H, H-N aniline), 8.43 (s, 1H, H-C₂ quinazoline), 8.22 (s, 1H, H-C₅ quinazoline), 7.88 (s, 1H, H-C₂ aniline), 7.64 (d, J=9.5 Hz, 1H, H-C₆ aniline), 7.59 (s, 1H, H-C₈ quinazoline), 7.26 (t, J=10 Hz, 1H, H-C₅ aniline), 7.18 (s, 1H, H-C₄ aniline), 4.21 (s, 2H, OCH₂), 3.95 (s, 3H, OCH₃), 2.92 (s, 2H, NCH₂), 2.64 (d, J=7 Hz, 4H, CH₂ diethylamine), 2.33 (s, 3H, CH₃ aniline), 1.01 (t, J=6.5 Hz, 6H, CH₃ diethylamine). ¹³CNMR (DMSO-*d*₆, 125 MHz) δppm 157.0, 153.5, 147.5, 140.1, 138.1, 128.8, 124.6, 123.4, 120.1, 109.5, 108.4, 107.0, 102.9, 73.1, 67.6, 57.0, 51.4, 47.6, 21.7, 12.2. MS (ESI): m/z 380 [M+H]⁺. Anal. Calcd for C₂₂H₂₈N₄O₂: C, 69.45; H, 7.42; N, 14.73. Found: C, 69.18; H, 7.43; N, 14.76.

7-(2-morpholinoethoxy)-N-(4-bromo-2-fluorophenyl)-6-methoxyquinazolin-4-amine (8e)

Yield: 39%; mp=196-197°C; IR (KBr, cm⁻¹) v_{max}: 3410 (NH aniline), 1475 (CH₂O), 1290 (CH₃O). ¹HNMR (DMSO-*d*₆, 500 MHz): δppm 9.57 (s, 1H, H-N aniline), 8.32 (s, 1H, H-C₂ quinazoline), 7.79 (s, 1H- H-C₅ quinazoline), 7.63 (d, J=10 Hz, 1H, H-C₃ aniline), 7.50 (t, J=8 Hz, 1H, H-C₅ aniline), 7.44 (d, J=8 Hz, 1H,

H-C₆ aniline), 7.19(s, 1H, H-C₈ quinazoline), 4.23 (brs, 2H, OCH₂), 3.91 (s, 3H, OCH₃), 3.56 (brs, 4H, H-C_{3,5} morpholine), 2.74 (brs, 2H, NCH₂), 2.47 (brs, 4H, H-C_{2,6} morpholine). ¹³CNMR (DMSO-*d*₆, 125 MHz) δppm 157.5, 154.2, 153.5, 147.5, 130.1, 128.0, 128.1, 120.0, 119.8, 109.3, 108.5, 108.4, 102.7, 102.8, 67.0, 66.8, 57.3, 56.8, 54.2. MS (ESI): m/z 476.2 [M+H]⁺. Anal. Calcd for C₂₁H₂₂BrFN₄O₂: C, 52.84; H, 4.65; N, 11.74. Found: C, 53.08; H, 4.66; N, 11.69.

7-(2-morpholinoethoxy) -N-(3-ethynylphenyl) -6-methoxyquinazolin-4-amine (8f)

Yield: 37%; mp=163-165°C; IR (KBr, cm⁻¹) v_{max}: 3410 (NH aniline), 1435 (CH₂O), 1237 (CH₃O), 2135 (ethynyl). ¹HNMR (DMSO-*d*₆, 500 MHz): δppm 9.66 (s, 1H, H-N aniline), 8.48(s, 1H, H-C₂ quinazoline), 8.02 (s, 1H, H-C₅ quinazoline), 7.94(s, 1H, H-C₄ aniline), 7.92 (s, 1H, H-C₂ aniline), 7.38(t, J=10 Hz, 1H, H-C₅ aniline), 7.22 (d, J=8.5 Hz, 1H, H-C₆ aniline), 7.18(s, 1H, H-C₈ quinazoline), 4.25 (t, J=5.5 Hz, 2H, OCH₂), 4.19 (s, 1H, CH ethynyl), 3.96 (s, 3H, OCH₃), 3.58 (brs, 4H, H-C_{3,5} morpholine), 2.76 (t, J=4.5 Hz, 2H, NCH₂), 2.72 (brs, 1H, CH ethynyl), 2.50 (brs, 4H, H-C_{2,6} morpholine). ¹³CNMR (DMSO-*d*₆, 125 MHz) δppm 156.7, 155.4, 153.2, 143.4, 140.5, 129.4, 126.8, 125.3, 123.2, 122.2, 109.6, 108.6, 102.8, 84.1, 81.0, 66.9, 66.7, 57.3, 57.0, 54.2. MS (ESI): m/z 404.3 [M+H]⁺. Anal. Calcd for C₂₃H₂₄N₄O₃: C, 68.30; H, 5.98; N, 13.85. Found: C, 68.47; H, 5.99; N, 13.78.

7-(2-morpholinoethoxy) -N-(3-fluorophenyl) -6-methoxyquinazolin-4-amine (8g)

Yield: 37%; mp=210.1-213°C; IR (KBr, cm⁻¹) v_{max}: 3459 (NH aniline), 1442 (CH₂O), 1228 (CH₃O). ¹HNMR (DMSO-*d*₆, 500 MHz): δppm 9.66 (s, 1H, H-N aniline), 8.52 (s, 1H, H-C₂ quinazoline), 7.92 (s, 1H, H-C₅ quinazoline), 8.89 (s, 1H, H-C₂ aniline), 7.64 (d, J=7.5 Hz, 1H, H-C₄ aniline), 7.41 (brs, 1H, H-C₅ aniline), 7.24 (d, J=8.5Hz, 1H, H-C₆ aniline), 6.91 (s, 1H, H-C₈ quinazoline), 4.26 (brs, 2H, OCH₂), 3.97 (s, 3H, OCH₃), 3.59 (brs, 4H, H-C_{3,5} morpholine), 2.78 (brs, 2H, NCH₂), 2.50 (brs, 4H, H-C_{2,6} morpholine). ¹³CNMR (DMSO-*d*₆, 125 MHz) δppm 157.0, 156.7, 154.2, 154.1, 153.2, 140.9, 130.5, 130.4, 118.0, 109.2, 109.0, 108.7, 102.7, 102.8, 67.0, 66.8, 57.3, 57.0, 54.2. MS (ESI): m/z 398.3 [M+H]⁺. Anal. Calcd for C₂₁H₂₃FN₄O₃: C, 63.30; H, 5.82; N, 14.06. Found: C, 63.14; H, 5.84; N, 14.12.

7-(2-morpholinoethoxy)-6-methoxy-N-m-tolylquinazolin-4-amine (8h)

Yield: 37%; mp=143.2-144.7°C; IR (KBr, cm⁻¹) v_{max}: 3327 (NH aniline), 1493 (CH₂O), 1275 (CH₃O). ¹HNMR (DMSO-*d*₆, 500 MHz): δppm 9.83 (s, 1H, H-N aniline), 8.52(s, 1H, H-C₂ quinazoline), 8.31 (s, 1H, H-C₅ quinazoline), 8.28 (t, J=8 Hz, 1H, H-C₄ aniline), 7.93 (s, 1H, H-C₂ aniline), 7.62 (t, J=8 Hz, 1H, H-C₅ aniline), 7.44 (d, J=7.6 Hz, 1H, H-C₆ aniline), 7.25 (s, 1H, H-C₈ quinazoline), 4.27 (t, J=5.5 Hz, 2H, OCH₂), 3.98 (s, 3H, OCH₃), 3.59 (brs, 4H, H-C_{3,5} morpholine), 2.78 (t, J=4.5 Hz, 2H, NCH₂), 2.50 (brs, 4H, H-C_{2,6} morpholine), 2.33(s, 3H, CH₃ aniline). ¹³CNMR (DMSO-*d*₆, 125 MHz) δppm 156.7, 154.2, 153.1, 147.8, 142.5, 141.1, 130.1, 125.9, 119.8, 118.6, 118.4, 108.6, 102.8, 102.7, 67.0, 66.8, 57.3, 57.0, 54.2. MS (ESI): m/z 448.4 [M+H]⁺. Anal. Calcd for C₂₂H₂₆N₄O₃: C, 66.99; H, 6.64; N, 14.20. Found: C, 67.13; H, 6.66; N, 14.16.

7-(2-(4-methylpiperazin-1-yl)ethoxy) -N-(4-bromo-2-fluorophenyl)-6-methoxyquinazolin-4-amine (8i)

Yield: 38%; mp=227.8-230°C; IR (KBr, cm⁻¹) v_{max}: 3410 (NH aniline), 1424 (CH₂O), 1282 (CH₃O). ¹HNMR (DMSO-*d*₆, 500 MHz): δppm 9.54 (s, 1H, H-N aniline), 8.35 (s, 1H, H-C₂ quinazoline), 8.20 (s, 1H, H-C₅ quinazoline), 7.79 (s, 1H, H-C₂ aniline), 7.66 (d, J= 7.5 Hz, 1H, H-C₆ aniline), 7.47 (brs, 1H, H-C₅ aniline), 7.22 (s, 1H, H-C₈ quinazoline), 4.24 (s, 2H, OCH₂), 3.93 (s, 3H, OCH₃), 2.76 (brs, 2H, NCH₂), 2.54 (brs, 4H, H-C_{3,5} piperazine), 2.35(brs, 4H, H-C_{2,6} piperazine), 2.16 (s, 3H, NCH₃). ¹³CNMR (DMSO-*d*₆, 125 MHz) δppm 157.4, 157.2, 153.5, 150.3, 150.1, 145.3, 143.5, 138.4, 135.3, 130.6, 130.0, 128.0, 123.6, 108.5, 97.6, 56.9, 56.7, 55.3, 53.6, 46.2, 42.4. MS (ESI): m/z 491 [M+H]⁺. Anal. Calcd for C₂₂H₂₅BrFN₅O₂: C, 53.89; H, 5.14; N, 14.28. Found: C, 54.13; H, 5.13; N, 14.30.

7-(2-(4-methylpiperazin-1-yl)ethoxy)-N-(3-ethynylphenyl) -6-methoxyquinazolin-4-amine (8j)

Yield: 35%; mp=217.3-220°C; IR (KBr, cm⁻¹) v_{max}: 3398 (NH aniline), 1453 (CH₂O), 1237 (CH₃O), 2160 (ethynyl). ¹HNMR (DMSO-*d*₆, 500 MHz): δppm 9.57 (s, 1H, H-N aniline), 8.50 (s, 1H, H-C₂ quinazoline), 8.01 (s, 1H, H-C₅ quinazoline), 7.91 (d, J=9 Hz, 1H, H-C₆ aniline), 7.88 (s, 1H, H-C₂ aniline), 7.40 (t, J=7 Hz, 1H, H-C₅ aniline), 7.22 (s, 1H, H-C₈ quinazoline), 7.20 (brs,

1H, H-C₄ aniline), 4.24 (brs, 2H, OCH₂), 4.20 (s, 1H, CH ethynyl), 3.97 (s, 3H, OCH₃), 2.76 (brs, 2H, NCH₂), 2.54 (brs, 4H, H-C_{3,5} piperazine), 2.34 (brs, 4H, H-C_{2,6} piperazine), 2.15 (s, 3H, NCH₃). ¹³CNMR (DMSO-*d*₆, 125 MHz) δppm 154.4, 153.3, 147.5, 140.6, 129.4, 126.8, 125.3, 123.1, 122.1, 121.7, 109.6, 108.7, 102.7, 81.0, 67.2, 59.9, 56.9, 55.3, 53.6, 46.3. MS (ESI): m/z 417.0 [M+H]⁺. Anal. Calcd for C₂₄H₂₇N₅O₂: C, 69.04; H, 6.52; N, 16.77. Found: C, 69.35; H, 6.53; N, 16.70.

7-(2-(4-methylpiperazin-1-yl)ethoxy)-N-(3-fluorophenyl)-6-methoxyquinazolin-4-amine (8k)

Yield: 41%; mp=215-216.3°C; IR (KBr, cm⁻¹) v_{max}: 3437 (NH aniline), 1480 (CH₂O), 1310 (CH₃O). ¹HNMR (DMSO-*d*₆, 500 MHz): δppm 9.65 (s, 1H, H-N aniline), 8.51 (s, 1H, H-C₂ quinazoline), 8.22 (s, 1H, H-C₅ quinazoline), 7.91 (s, 1H, H-C₂ aniline), 7.88 (brs, 1H, H-C₄ aniline), 7.63 (d, J=7 Hz, 1H, H-C₆ aniline), 7.40 (d, J=7 Hz, 1H, H-C₅ aniline), 7.23(s, 1H, H-C₈ quinazoline), 4.24(brs, 2H, OCH₂), 3.97 (s, 3H, OCH₃), 2.77 (brs, 2H, NCH₂), 2.54 (brs, 4H, H-C_{3,5} piperazine), 2.40 (brs, 4H, H-C_{2,6} piperazine), 2.19 (s, 3H, NCH₃). ¹³CNMR (DMSO-*d*₆, 125 MHz) δppm 159.6, 153.2, 149.7, 147.6, 147.5, 130.4, 130.3, 118.0, 110.0, 109.9, 109.2, 109.0, 108.7, 102.7, 67.2, 57.0, 56.8, 55.1, 53.3, 46.0. MS (ESI): m/z 411.3 [M+H]⁺. Anal. Calcd for C₂₂H₂₆FN₅O₂: C, 64.22; H, 6.37; N, 17.02. Found: C, 64.05; H, 6.39; N, 17.04.

7-(2-(4-methylpiperazin-1-yl)ethoxy) -6-methoxy -N-methylquinazolin-4-amine (8l)

Yield: 35%; mp=237.3-240°C; IR (KBr, cm⁻¹) v_{max}: 3315 (NH aniline), 1470 (CH₂O), 1297 (CH₃O). ¹HNMR (DMSO-*d*₆, 500 MHz): δppm 9.57 (s, 1H, H-N aniline), 8.51 (s, 1H, H-C₂ quinazoline), 8.03 (s, 1H, H-C₅ quinazoline), 7.83 (s, 1H, H-C₂ aniline), 7.80 (d, J=8 Hz, 1H, H-C₆ aniline), 7.41 (t, J=8.5 Hz, 1H, H-C₅ aniline), 7.22 (s, 1H, H-C₈ quinazoline), 7.15 (d, J=9 Hz, 1H, H-C₄ aniline), 4.24 (brs, 2H, OCH₂), 3.96 (s, 3H, OCH₃), 2.79 (s, 2H, NCH₂), 2.54 (brs, 4H, H-C_{3,5} piperazine), 2.37 (brs, 4H, H-C_{2,6} piperazine), 3.33 (s, 3H, H-CH₃ C₃ aniline), 2.17 (s, 3H, NCH₃). ¹³CNMR (DMSO-*d*₆, 125 MHz) δppm 158.8, 155.6, 151.7, 148.2, 144.0, 130.6, 126.6, 115.7, 109.8, 107.2, 102.4, 95.7, 88.5, 79.6, 57.6, 56.4, 54.8, 50.9, 46.8, 22.1. MS (ESI): m/z 407 [M+H]⁺. Anal. Calcd for C₂₃H₂₉N₅O₂: C, 67.79; H, 7.17; N, 17.19. Found: C, 67.93; H, 7.18; N, 17.26.

MTT Cell Viability Assay

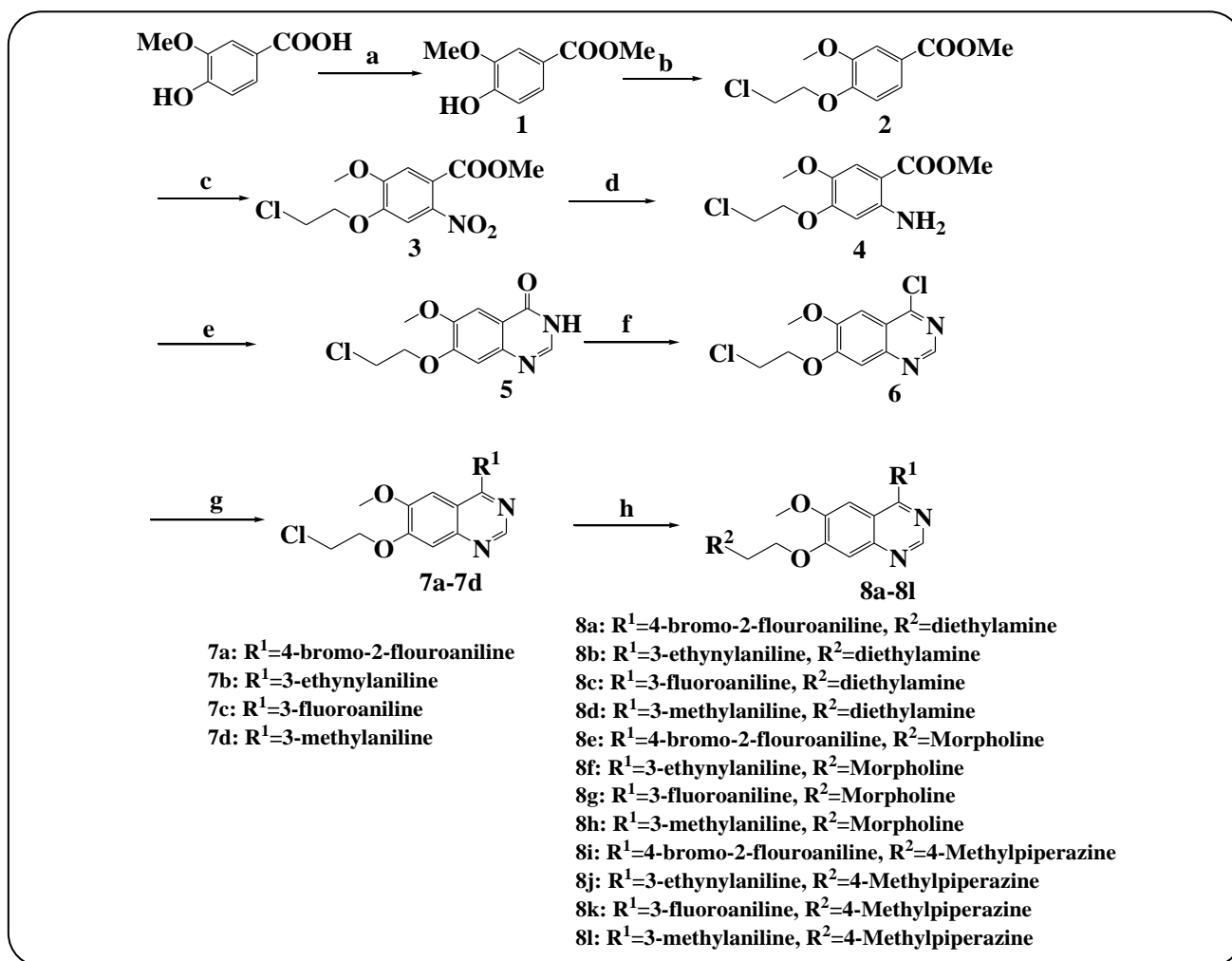
The viability of A431 human skin cancer (Epidermoid carcinoma) and HU02 (human foreskin fibroblast) cell lines were determined by MTT assay as described previously [2,34-40]. Basically, cells were seeded in 96-well plates at a density of 5×10³ per well and incubated at 37°C in a humidified atmosphere with 5% CO₂ for 24h. The cells were treated with erlotinib, vandetanib, and synthesized compounds (**8a-8l**) at various concentrations (1, 2, 5, 10, 20, 50, 100, and 200 μM) which were prepared by dissolving them in 0.1% DMSO and diluted with the medium. The solvent was used as a negative control. MTT solution (Sigma; 5mg/mL of PBS) was added to each well 72 hours after treatment, and the cells were incubated for 3 hours at 37°C. Then, the supernatant was discarded; 150 μL DMSO was added to each well, and absorbance was measured using a Biotek Epoch™ microplate reader at 570 nm.

Statistical Analysis:

All experiments were done in triplicate and IC₅₀ values were calculated by nonlinear regression with normalized dose-response fit using GraphPad Prism® version 5 and expressed as mean ± Standard Deviation (S.D.) in μM (GraphPad Software., Inc. San Diego, CA) [41].

Molecular Docking

Compounds **8a** and vandetanib were chosen for molecular docking with EGFR and VEGFR2. Docking study was done using AutoDock 4.2 and AutoDock Tools 1.5.4 (ADT) [18,24,35,42-45]. The X-ray crystal structure of EGFR tyrosine kinase domain with 4-anilinoquinazoline inhibitor erlotinib (PDB ID: 1M17) and crystal structure of the VEGFR2 kinase domain in complex with a 2,3-dihydro-1,4-benzoxazine inhibitor (PDB ID: 2RL5) was downloaded from the protein data bank (<http://www.rcsb.org>). Ligand and water molecules were removed from crystal structures of receptors followed by adding hydrogens and Kollman charges and merging non-polar hydrogens. Structures of previously mentioned compounds were drawn and the molecular geometries were optimized by molecular mechanics MM+ and then semi-empirical AM1 methods using HyperChem 8.0 software. During docking studies, ligand bonds were set free, while EGFR and VEGFR were kept rigid. Grid box dimensions were set to x=90, y=90, z=90 along with grid spacing of 0.375 Å. The Lamarckian genetic search



Scheme 1: Synthetic route for the synthesis of the target compounds **8a–8l**. Reagents and conditions: (a) $\text{SOCl}_2, \text{MeOH}$, Reflux; (b) 1-Bromo-2-chloroethane, TBAB, K_2CO_3 , Reflux; (c) H_2SO_4 , HNO_3 , 0–5 °C; (d) Fe, NH_4Cl , $\text{MeOH}/\text{H}_2\text{O}$, Reflux; (e) formamidineacetate, Ethanol, Reflux; (f) Oxalyl chloride, DMF, Dichloromethane, rt; (g) Aniline Derivatives, *i*-PrOH, Reflux; (h) KI, DMF, Secondary amine, Reflux.

the algorithm was utilized with 100 GA runs. Validation of the docking procedure was done using co-crystallized ligands based on the method mentioned earlier.

RESULTS AND DISCUSSION

A novel series of 4-anilinoquinazoline derivatives bearing various secondary amine derivatives including methylpiperazine, morpholine, and diethylamine at C-7 position along with various substituted aniline rings at C-4 position of quinazoline core was synthesized, characterized by IR, NMR, mass spectroscopy and elemental analysis methods. The synthetic pathway is shown in scheme 1. Intermediate **1** was synthesized by the esterification of vanillic acid with thionyl chloride in

methanol. The reaction of 1-bromo-2-chloroethane in the presence of potassium carbonate and TBAB with **1** afforded intermediate **2**. The nitration process of **2** was done using sulfuric acid and nitric acid to obtain **3**. Then, compound **3** was reduced to **4** by ammonium chloride and powdered iron followed by the closure of the quinazoline ring in the presence of formamidine acetate in ethanol to achieve **5** [10,24–28]. Chlorination of **5** by oxalyl chloride yielded the intermediate **6** [26,28,29]. The coupling of **6** with the proper anilines yielded compounds **7a–7d** [10,30]. Finally, the reaction of **7a–7d** with different secondary amine derivatives in the presence of anhydrous potassium iodide gave the target compounds **8a–8l** [24,31–33].

The synthesized compounds were tested for *in-vitro* cytotoxicity against A431 and HU02 cell lines using the MTT assay [2,34-38]. Erlotinib is an EGFR tyrosine kinase inhibitor and vandetanib as a dual inhibitor of EGFR and VEGFR-2 were used as positive controls in this assay. The biological results were represented as the IC₅₀ values (the concentration needed for 50% inhibition of cell survival) in Table 1.

Most compounds indicated significant cytotoxic activity with IC₅₀ values lower than 100 μM with the exception of **8e**, **8h**, and **8i**. Surprisingly, **8a** bearing diethylamine at C-7 position along with 4-bromo-2-fluoroaniline at C-7 position of quinazoline ring showed the best cytotoxicity against A431 cell line (IC₅₀=2.62 μM) which was better than positive controls (Erlotinib: IC₅₀=8.31 μM and Vandetanib: IC₅₀=10.62 μM). Replacement of the 4-bromo-2-fluoroaniline in **8a** with other aniline derivatives including 3-ethynylaniline (**8b**), 3-fluoroaniline (**8c**), and 3-methylaniline (**8d**) with IC₅₀ values of 50.97 μM, 50.98 μM, and 21.65 μM, respectively, led to a dramatic drop of cytotoxic activity. The compound **8k** (IC₅₀=19.23 μM) was classified as another potent agent bearing N-methylpiperazine at 7-position and 3-fluoroaniline at 4-position of quinazoline moiety. As is presented, on replacing 3-fluoroaniline of **8k** with 3-methylaniline (**8l**), 3-ethynylaniline (**8j**), and 4-bromo-2-fluoroaniline (**8i**) the cytotoxicity was significantly decreased. The IC₅₀ values of derivatives with morpholine substituent at 7-position of quinazoline nucleus indicated that **8f** bearing 3-ethynylaniline (IC₅₀=42.96 μM) and **8g** with 3-fluoroaniline (IC₅₀=37.25 μM) were the best compounds within this group. Compounds **8e** and **8h** did not show acceptable cytotoxic activities against A431 in comparison with erlotinib and vandetanib (IC₅₀>100). By investigating the structural modifications and the IC₅₀ values of synthesized compounds, it can be concluded that the conformational flexibility, as well as decreasing steric hindrance of diethylamine moiety, might enhance the inhibitory activity. Also, higher lipophilicity of diethylamine compared to morpholine and N-methylpiperazine may improve cell penetration, which leads to higher cytotoxicity. Interestingly, tested compounds did not show significant cytotoxicity against HU02 cells.

Moreover, a docking study was done to investigate the interactions of the most potent final derivatives including **8a** and vandetanib with the active site of the

EGFR-TK and VEGFR2 receptors and validated using the active conformation of the co-crystal ligands. PDB ID: 1M17 and 2RL5 were chosen as the target protein with co-crystal ligands (Table 2) [18,24,35,42-44].

For the EGFR-TK receptor, the aniline groups of **8a** and vandetanib formed predominantly hydrophobic interactions with residues in the hydrophobic pocket, including **Leu694**, **Val702**, and **Ala719**. In addition, the critical interaction between these structures and the EGFR was a hydrogen bond that was formed between the residue **Met769** and the quinazoline N1 of both compounds (**8a**: 1.713 Å, vandetanib: 1.945 Å) (Figure 3). These interactions are essential for anchoring quinazoline derivatives in the ATP-binding cleft of the EGFR. Both compounds were found to be best fitted in the ATP binding site of EGFR that showed fairly appropriate binding energies of -6.39 and -7.72 kcal/mol as well as inhibition constants of 20.67 μM and 2.21 μM for compound **8a** and vandetanib, respectively.

The binding study of **8a** and vandetanib with VEGFR depicted that one critical H-bond formed between the backbone amino acid residue **Cyc919** of VEGFR-2 and quinazoline N1 atom with the distances of 2.809 Å and 2.12 Å, respectively. Also, **8a** has bifurcated hydrogen bonds created via interaction of quinazoline N3 atom with **Phe918** and **Thr916**. The compound **8a** and vandetanib depicted binding energies of -8.24 and -8.97 kcal/mol as well as inhibition constants of 0.9 μM and 0.26 μM, respectively, which indicated the effective binding with VEGFR-2. The higher potency of **8a** may be attributed to shorter hydrogen bond distance along with forming additional hydrogen bonds (Fig. 4).

CONCLUSIONS

Several quinazoline derivatives bearing secondary amines containing dimethylamine, morpholine, and N-methylpiperazine C-7 position, as well as different substituted aniline rings at and C-4 position of quinazoline scaffold, were designed, synthesized, and characterized by different methods including IR, ¹HNMR, ¹³CNMR, Mass spectroscopy, and elemental analysis. Synthesized derivatives were investigated as anticancer agents against A431 and HU02 cell lines by MTT assay. Most compounds had significant cytotoxic activities on A431 cells with overexpressed EGFR. Among them, **8a**, **8d**, and **8k** indicated significant inhibitory activity in comparison

Table 1: In vitro antiproliferative activity of compounds 8a–8l in A431 and HU02 cell lines.

Compounds	R ¹	R ²	IC ₅₀ (μM)±μM	
			A431	HU02
8a			2.62±0.54	>100
8b			50.97±6.43	>100
8c			50.98±7.71	>100
8d			21.65±3.33	>100
8e			>100	>100
8f			42.96±6.27	>100
8g			37.25±4.87	>100
8h			>100	>100
8i			>100	>100
8j			81.07±9.12	>100
8k			19.23±2.94	>100
8l			75.92±8.23	>100
Erlotinibe hydrochloride			8.31±1.96	
Vandetanib			10.62±2.54	

Table 2: The binding energies, inhibition constants, and number of hydrogen bond interactions of 8a for the binding site of EGFR and VEGFR.

Macromolecule	Ligand	Binding energy (kcal/ mol)	Ki (μ M)	Number of hydrogen bond interactions
EGFR	8a	-6.39	20.67	1
	Vandetanib	-7.72	2.21	1
VEGFR-2	8a	-8.24	0.90	2
	Vandetanib	-8.97	0.26	1

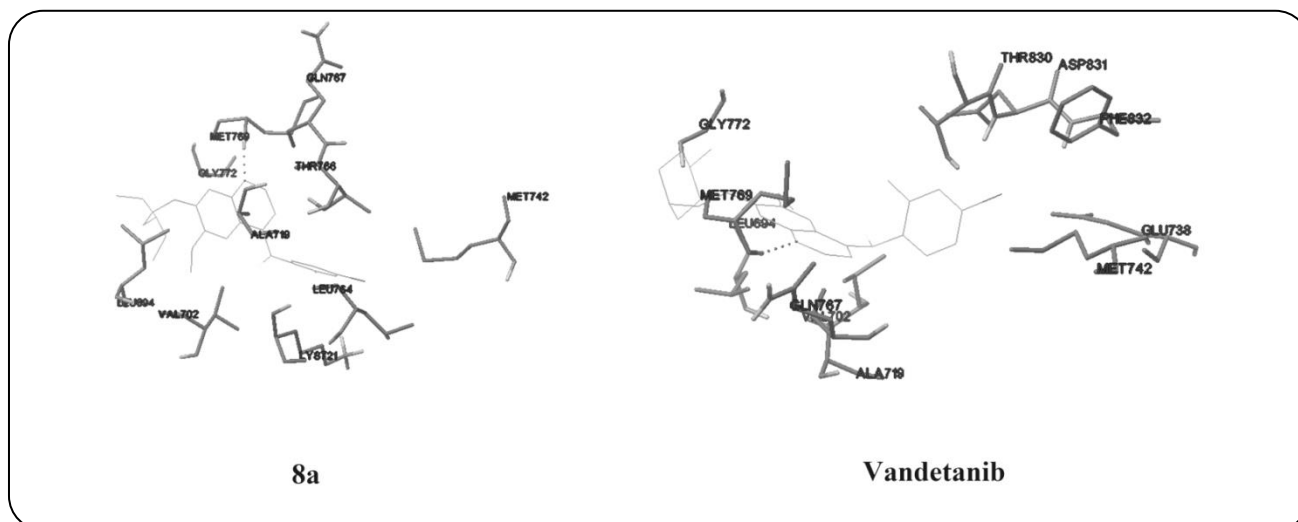


Fig. 3: Docking interaction of compound 8a and vandetanib with EGFR.

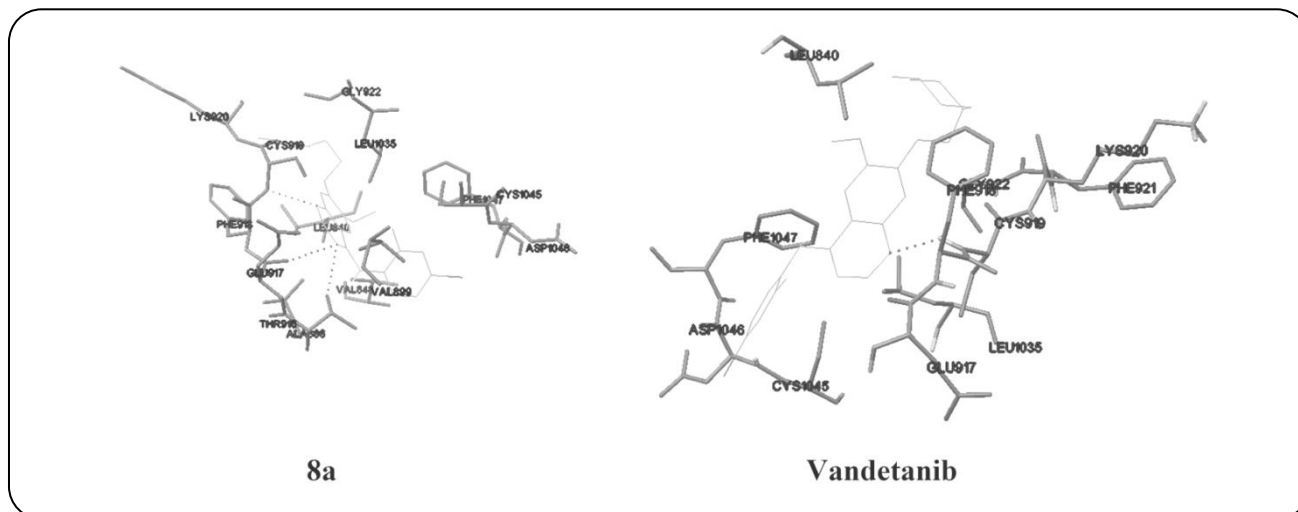


Fig. 4: Docking interaction of compound 8a and vandetanib with VEGFR2.

with erlotinib and vandetanib as positive controls. Cytotoxic activity of **8a** with diethylamine and 4-bromo-2-fluoroaniline was better than standards while **8d** and **8k** showed lower potency than positive controls. The better cytotoxic activity of diethylamine derivatives may be attributed to

higher lipophilicity, and flexibility along with the lower hindrance of diethylamine. The compound **8a** was placed in the active site of EGFR and VEGFR properly via the formation of hydrogen bonding of quinazoline N1 and hydrophobic interaction of the aniline ring. Cytotoxicity

results against A431 were in line with the results of docking studies on both EGFR and VEGFR2. All tested compounds did not exhibit measurable cytotoxic activity on HU02. These results proved that mentioned compounds could be useful for further investigation and optimization to synthesize more potent derivatives.

Acknowledgments

This work was supported by the Guilan University of Medical Sciences. This study was approved by the Ethical Committee of Guilan University of Medical Sciences (ID: IR. GUMS. REC. 1397.132, Date: 23. June. 2018).

Received : Aug. 9, 2020 ; Accepted : Oct. 26, 2020

REFERENCES

- [1] Antonello A., Tarozzi A., Morroni F., Cavalli A., Rosini M., Hrelia P., Bolognesi M.L., Melchiorre C., **Multitarget-Directed Drug Design Strategy: A Novel Molecule Designed to Block Epidermal Growth Factor Receptor (EGFR) and to Exert Proapoptotic Effects**, *J. Med. Chem.*, **49(23)**:6642-6645 (2006).
- [2] Ghasemi S., Sharifi S., Davaran S., Danafar H., Asgari D., Mojarrad J.S., **Synthesis and Cytotoxicity Evaluation of Some Novel 1-(3-Chlorophenyl) Piperazin-2-one Derivatives Bearing Imidazole Bioisosteres**, *Aust. J. Chem.*, **66(6)**: 655-660 (2013).
- [3] Torre L.A., Bray F., Siegel R.L., Ferlay J., Lortet-Tieulent J., Jemal A., **Global Cancer Statistics, 2012**, *CA Cancer J. Clin.*, **65(2)**:87-108 (2015).
- [4] Aliabadi A., Fereidooni R., Kiani A., **Synthesis and Cytotoxicity Evaluation of N-(5-(Substituted-Benzylthio)-1, 3, 4-Thiadiazole-2-yl)-2-p-Nitrophenylacetamide Derivatives as Potential Anticancer Agents**, *Iran. J. Chem. Chem. Eng. (IJCCE)*, **38(1)**: 49-55 (2019).
- [5] Yinhuo D., Froughi M.M., Aramesh-Boroujeni Z., Jahani S., Peydayesh M., Borhani F., Khatami M., Rohani M., Dusek M., Eigner V., **The Synthesis, Characterization, DNA/BSA/HSA Interactions, Molecular Modeling, Antibacterial Properties, and In Vitro Cytotoxic Activities of Novel Parent and Niosome Nano-Encapsulated Ho (III) Complexes**, *RSC Adv.*, **10(39)**: 22891-22908 (2020).
- [6] Aliabadi A., Afanzade N.-S., Hosseinzadeh L., Mohammadi-Farani A., Shafiee M.H., Nazari H., Ahmadi F., Foroumadi A.R., **N-(5-(Trifluoromethyl)-1, 3, 4-Thiadiazol-2-yl) Benzamide and Benzothioamide Derivatives Induce Apoptosis via Caspase-Dependent Pathway**, *Pharm. Chem. J.*, **53(6)**: 521-526 (2019).
- [7] Manikala V., **Synthesis, Molecular Docking and Anticancer Activity of Novel (E)-5-((1-Phenyl-1H-1, 2, 3-Triazol-4-yl) Methylene)-2-Thioxothiazolidin-4-one Analogues**, *Iran. J. Chem. Chem. Eng. (IJCCE)*, **40(6)**: 1793- 1799 (2021).
- [8] Li S., Guo C., Sun X., Li Y., Zhao H., Zhan D., Lan M., Tang Y., **Synthesis and Biological Evaluation of Quinazoline and Quinoline Bearing 2, 2, 6, 6-Tetramethylpiperidine-N-Oxyl as Potential Epidermal Growth Factor Receptor (EGFR) Tyrosine Kinase Inhibitors and EPR Bio-Probe Agents**, *Eur. J. Med. Chem.*, **49**: 271-278 (2012).
- [9] Wee P., Wang Z., **Epidermal Growth Factor Receptor Cell Proliferation Signaling Pathways**, *Cancers*, **9(5)**: 52-97 (2017).
- [10] Li R.-D., Zhang X., Li Q.-Y., Ge Z.-M., Li R.-T., **Novel EGFR Inhibitors Prepared by Combination of Dithiocarbamic Acid Esters and 4-Anilinoquinazolines**, *Bioorg. Med. Chem.*, **21(12)**: 3637-3640 (2011).
- [11] Sarfraz M., Rashid U., Sultana N., Tariq M.I., **Synthesis, X-Rays Analysis, Docking Study and Cholinesterase Inhibition Activity of 2, 3-Dihydroquinazolin-4 (1H)-One Derivatives**, *Iran. J. Chem. Chem. Eng. (IJCCE)*, **38(6)**: 213-227 (2019).
- [12] Sun M., Jia J., Sun H., Wang F., **Design and Synthesis of a Novel Class EGFR/HER2 Dual Inhibitors Containing Tricyclic Oxazine Fused Quinazolines Scaffold**, *Bioorg. Med. Chem.*, **30(9)**:1-6 (2020).
- [13] Garofalo A., Goossens L., Lemoine A., Ravez S., Six P., Howsam M., Farce A., Depreux P., **[4-(6, 7-Disubstituted Quinazolin-4-ylamino) Phenyl] Carbamic Acid Esters: A Novel Series of Dual EGFR/VEGFR-2 Tyrosine Kinase Inhibitors**, *MedChemComm*, **2(1)**: 65-72 (2011).
- [14] Sini P., Wyder L., Schnell C., O'Reilly T., Littlewood A., Brandt R., Hynes N.E., Wood J., **The Antitumor and Antiangiogenic Activity of Vascular Endothelial Growth Factor Receptor Inhibition is Potentiated by ErbB1 Blockade**, *Clin. Cancer Res.*, **11(12)**: 4521-4532 (2005).

- [15] Garofalo A., Goossens L., Six P., Lemoine A., Ravez S., Farce A., Depreux P., [Impact of Aryloxy-Linked Quinazolines: A Novel Series of Selective VEGFR-2 Receptor Tyrosine Kinase Inhibitors](#), *Bioorg. Med. Chem.*, **21**(7): 2106-2112 (2011).
- [16] Xu P., Chu J., Li Y., Wang Y., He Y., Qi C., Chang J., [Novel Promising 4-Anilinoquinazoline-Based Derivatives as Multi-Target RTKs Inhibitors: Design, Molecular Docking, Synthesis, and Antitumor Activities In Vitro and Vivo](#), *Bioorg. Med. Chem.*, **27**(20): 1-8 (2019).
- [17] Ismail R.S.M., Abou-Seri S.M., Eldehna W.M., Ismail N.S.M., Elgazwi S.M., Ghabbour H.A., Ahmed M.S., Halaweish F.T., Abou El Ella D.A., [Novel Series of 6-\(2-Substitutedacetamido\)-4-Anilinoquinazolines as EGFR-ERK Signal Transduction Inhibitors in MCF-7 Breast Cancer Cells](#), *Eur. J. Med. Chem.*, **155**:782-796 (2018).
- [18] Wei H., Duan Y., Gou W., Cui J., Ning H., Li D., Qin Y., Liu Q., Li Y., [Design, Synthesis and Biological Evaluation of Novel 4-Anilinoquinazoline Derivatives as Hypoxia-Selective EGFR and VEGFR-2 Dual Inhibitors](#), *Eur. J. Med. Chem.*, **181**(1):1-12 (2019).
- [19] Hennequin L.F., Stokes E.S., Thomas A.P., Johnstone C., Plé P.A., Ogilvie D.J., Dukes M., Wedge S.R., Kendrew J., Curwen J.O., [Novel 4-Anilinoquinazolines with C-7 Basic Side Chains: Design and Structure-Activity Relationship of a Series of Potent, Orally Active, VEGF Receptor Tyrosine Kinase Inhibitors](#), *J. Med. Chem.*, **45**(6):1300-1312 (2002).
- [20] Hennequin L.F., Thomas A.P., Johnstone C., Stokes E.S., Plé P.A., Lohmann J.-J.M., Ogilvie D.J., Dukes M., Wedge S.R., Curwen J.O., Kendrew J., van der Brempt Ch.L., [Design and Structure-Activity Relationship of a New Class of Potent VEGF Receptor Tyrosine Kinase Inhibitors](#), *J. Med. Chem.*, **42**(26):5369-5389 (1999).
- [21] Zhang H.-Q., Gong F.-H., Li C.-G., Zhang C., Wang Y.-J., Xu Y.-G., Sun L.P., [Design and Discovery of 4-Anilinoquinazoline-Acylamino Derivatives as EGFR and VEGFR-2 Dual TK Inhibitors](#), *Eur. J. Med. Chem.*, **109**:371-379 (2016).
- [22] Eweas A.F., Maghrabi I.A., Namarneh A.I., [Advances in Molecular Modeling and Docking as a Tool for Modern Drug Discovery](#), *Der Pharma Chem.*, **6**(6):211-228 (2014).
- [23] Zhao M., Wang L., Zheng L., Zhang M., Qiu C., Zhang Y., Du D., Niu B., [2D-QSAR and 3D-QSAR Analyses for EGFR Inhibitors](#), *Biomed Res. Int.*, 2017 (2017).
- [24] Zhao F., Lin Z., Wang F., Zhao W., Dong X., [Four-Membered Heterocycles-Containing 4-Anilino-Quinazoline Derivatives as Epidermal Growth Factor Receptor \(EGFR\) Kinase Inhibitors](#), *Bioorg. Med. Chem.*, **23**(19):5385-5388 (2013).
- [25] Heydari Alizadeh B., Vosooghi M., Khoobi M., Javidnia A., Panah F., Safavi M., Adrestani S., Shafiee A., [Synthesis and Cytotoxic Activity of Novel 9-\[Hydroxy \(Substituted Phenyl\) Methyl\]-2, 2-Dimethyl-2, 3, 8, 9-Tetrahydro-4H, 10H-Pyrano \[2, 3-f\] Chromene-4, 10-Diones](#), *Iran. J. Chem. Chem. Eng. (IJCCE)*, **29**(4):189-196 (2010).
- [26] Holladay M.W., Campbell B.T., Rowbottom M.W., Chao Q., Sprankle K.G., Lai A.G., Abraham S., Setti E., Faraoni R., Tran L., Armstrong R.C., Gunawardane R.N., Gardner M.F., Cramer M.D., Gitnick D., Ator M.A., Dorsey B.D., Ruggeri B.R., James J., [4-Quinazolinyl-oxo-diaryl Ureas as Novel BRAFV600E Inhibitors](#), *Bioorg. Med. Chem.*, **21**(18): 5342-5346 (2011).
- [27] Mozaffari S., Ghasemi S., Baher H., Khademi H., Amini M., Sakhteman A., Foroumadi A., Ebrahimabadi A.H., Sharifzadeh M., [Synthesis and Evaluation of some Novel methylene-bridged Aryl Semicarbazones as Potential Anticonvulsant Agents](#), *Medicinal Chemistry Research*, **21**(11): 3797-3808 (2012).
- [28] Zhang N., Wu B., Powell D., Wissner A., Floyd M.B., Kovacs E.D., Toral-Barza L., Kohler C., [Synthesis and Structure-Activity Relationships of 3-cyano-4-\(phenoxyanilino\) Quinolines as MEK \(MAPKK\) Inhibitors](#), *Bioorg. Med. Chem.*, **10**(24): 2825-2828 (2000).
- [29] Ghasemi S., Sharifi S., Mojarrad J.S., [Design, Synthesis and Biological Evaluation of Novel Piperazinone Derivatives as Cytotoxic Agents](#), *Adv. Pharm. Bull.*, **10**(3):423-429 (2020).
- [30] Zhang Y., Gao H., Liu R., Liu J., Chen L., Li X., Zhao L., Wang W., Li B., [Quinazoline-1-deoxynojirimycin Hybrids as High Active Dual Inhibitors of EGFR and \$\alpha\$ -glucosidase](#), *Bioorg. Med. Chem.*, **27**(18): 4309-4313 (2017).

- [31] Garofalo A., Farce A., Ravez S.v., Lemoine A.I., Six P., Chavatte P., Goossens L., Depreux P., [Synthesis and Structure-Activity relationships of \(aryloxy\) quinazoline Ureas as Novel, Potent, and Selective Vascular Endothelial Growth Factor Receptor-2 Inhibitors](#), *J. Med. Chem.*, **55**(3):1189-1204 (2012).
- [32] Barker A.J., inventor; Zeneca Limited (London, GB2), Assignee. [Quinazoline Derivatives Useful for Treatment of Neoplastic Disease](#), *US Patent, 5457105* (1995).
- [33] Thomas A.P., Johnstone C., Hennequin L.F.A., inventors; Zeneca Limited (London, GB), Assignee. [4-anilinoquinazoline Derivatives](#), *US Patent 6291455* (2001).
- [34] Kondori T., Shahraki O., Akbarzadeh-T N., Aramesh-Boroujeni Z., [Two Novel Bipyridine-Based Cobalt \(II\) Complexes: Synthesis, Characterization, Molecular Docking, DNA-Binding and Biological Evaluation](#), *J. Biomol. Struct. Dyn.*:1-15 (2020).
- [35] Aramesh-Boroujeni Z., Aramesh N., Jahani S., Khorasani-Motlagh M., Kerman K., Noroozifar M., [Experimental and Computational Interaction Studies of Terbium \(III\) and Lanthanide \(III\) Complexes Containing 2, 2'-Bipyridine with Bovine Serum Albumin and Their *in Vitro* Anticancer and Antimicrobial Activities](#), *J. Biomol. Struct. Dyn.*:1-12 (2020).
- [36] Aramesh-Boroujeni Z., Jahani S., Khorasani-Motlagh M., Kerman K., Noroozifar M., [Parent and Nano-Encapsulated Ytterbium \(III\) Complex toward Binding with Biological Macromolecules, In Vitro Cytotoxicity, Cleavage and Antimicrobial Activity Studies](#), *RSC Adv.*, **10**(39): 23002-23015 (2020).
- [37] Hamidi M., Ghasemi S., Bavafa Bighdilou B., Eghbali Koochi D., [Evaluation of Antioxidant, Antibacterial and Cytotoxic Activity of Methanol Extract from Leaves and Fruits of Iranian Squirring Cucumber \(*Ecballium Elaterium* \(L.\) A. Rich\)](#), *Res. J. Pharmacogn. (RJP)*, **7**(1): 23-29 (2020).
- [38] Yousefbeyk F., Tabaside J., Ostad S., Salehi Sourmaghi M., Amin G., [Investigation of Chemical Composition and Cytotoxic Activity of Aerial Parts of *Ziziphora Clinopodioides* Lam](#), *Res. J. Pharmacogn. (RJP)*, **3**(2):47-51 (2016).
- [39] Zuo K., Qian J., Gong J., Zhang J., Li H., Zhou G., [Synthesis, Characterization, Molecular Docking and Cytotoxicity Studies of Bagasse Xylem Ferulate-Acrylamide/Methyl Methacrylate Composite](#), *Iran. J. Chem. Chem. Eng. (IJCCE)*, **38**(3): 107-116 (2019).
- [40] Ghasemi S., Davaran S., Sharifi S., [Comparison of Cytotoxic Activity of L778123 as a Farnesyltransferase Inhibitor and Doxorubicin Against A549 and HT-29 Cell Lines](#), *Adv. Pharm. Bull.*, **3**(1): 73 (2013).
- [41] Robichaux J.P., Elamin Y.Y., Tan Z., Carter B.W., Zhang S., Liu S., Li Sh., Chen T., Pottete A., Estrada-Bernal A., Le A.T., Truini A., Nilsson M.B., Sun H., Roarty E., Goldberg S.B., Brahmer J.R., Altan M., Lu Ch., Papadimitrakopoulou V., Politi K., Doebele R.C., Wong K.K., Heymach J.V., [Mechanisms and Clinical Activity of an EGFR and HER2 Exon 20-Selective Kinase Inhibitor in Non-Small Cell Lung Cancer](#), *Nat. Med.*, **24**(5): 638-646 (2018).
- [42] Meng F., [Molecular Dynamics Simulation of VEGFR2 with Sorafenib and Other Urea-Substituted Aryloxy Compounds](#), *J. Theor. Chem.*, **2013**:739574 (2013).
- [43] Aramesh-Boroujeni Z., Bordbar A.-K., Khorasani-Motlagh M., Fani N., Sattarinezhad E., Noroozifar M., [Computational and Experimental Study on the Interaction of Three Novel Rare Earth Complexes Containing 2, 9-Dimethyl-1, 10-Phenanthroline with Human Serum Albumin](#), *J. Iran. Chem. Soc.*, **15**(7): 1581-1591 (2018).
- [44] Aramesh-Boroujeni Z., Jahani S., Khorasani-Motlagh M., Kerman K., Noroozifar M., [Evaluation of Parent and Nano-Encapsulated Terbium \(III\) Complex toward its Photoluminescence Properties, FS-DNA, BSA Binding Affinity, and Biological Applications](#), *J. Trace Elem. Med. Biol.*, 126564 (2020).
- [45] Ibezim A.E., Onoabedje E.A., Akpomie K.G., [Docking and Biological Screening of Bezo \[A\] Phenothiazinones as Novel Inhibitors of Bacterial Peptidoglycan Transpeptidase](#), *Iran. J. Chem. Chem. Eng. (IJCCE)*, **38**(6):243-250 (2019).